CHAPTER 2

DYNAMIC SHEAR STRESS IN PARALLEL-PLATE FLOW CHAMBERS

Rommel G. Bacabac[1], Theo H. Smit[2], Stephen C. Cowin[3], Jack J.W.A. Van Loon[1,5], Frans T.M. Nieuwstadt[4], Rob Heethaar[2], Jenneke Klein-Nulend[1]

[1]Department of Oral Cell Biology, Academic Centre for Dentistry Amsterdam-Universiteit van Amsterdam and Vrije Universiteit, Amsterdam, The Netherlands

[2]Department of Physics and Medical Technology, VU University Medical Center, Amsterdam, The Netherlands

[3]Departments of Biomedical and Mechanical Engineering, The City College of New York, New York, NY, USA

[4]J.M. Burgers Centre, Delft University of Technology, Delft, The Netherlands

[5]Dutch Experiment Support Center, Vrije Universiteit, Amsterdam, The Netherlands

Journal of Biomechanics 38:159-167, 2005

ABSTRACT

An *in vitro* model using a parallel-plate fluid flow chamber is supposed to simulate *in vivo* fluid shear stresses on various cell types exposed to dynamic fluid flow in their physiological environment. The metabolic response of cells *in vitro*, is associated with the wall shear stress. However, parallel-plate flow chambers have not been characterized for dynamic fluid flow experiments. We use a dimensionless ratio h/λ_v, in determining the exact magnitude of the dynamic wall shear stress, with its oscillating components scaled by a *shear factor T*. It is shown that, in order to expose cells to predictable levels of dynamic fluid shear stress, two conditions have to be met: 1) $h/\lambda_v < 2$, where h is the distance between the plates and λ_v is the *viscous penetration depth*; and 2) $f_o < f_c / m$, where the *criticial frequency* f_c is the upper threshold for this flow regime, m is the highest harmonic mode of the flow, and f_o is the *fundamental frequency* of fluid flow.

INTRODUCTION

The parallel-plate flow chamber (PPFC) is used for flow stimulation of various cell types, *e.g.*, bone cells and endothelial cells (1). A cell monolayer attached to one of the internal plate surfaces is subjected to fluid flow by creating a pressure gradient along the chamber. To calculate the resulting shear stress on the cells, the mathematical model assumes a Newtonian fluid in which the shear tensor is proportional to the deformation tensor. For steady flow between infinitely wide parallel plates, wall shear stress τ_w is calculated as a function of the measured flow Q:

$$\tau_w = \frac{6\mu Q}{bh^2} \qquad [1]$$

with μ = fluid viscosity, b = width of the chamber, h = distance between plates. For finite chamber dimensions (finite b/h), the fluid velocity profile remains parabolic between the plates, but vanishes at the boundaries of the rectangular channel (Figure 1A, B) (2, 3). The shear stress profile, calculated from the velocity gradient, has maximum magnitudes at the plate surfaces and vanishes at the corners of the channel (Figure 1C). Less than 1% difference from a full parabolic velocity profile occurs after an entry length L_{entry} = 0.04hRe (Reynolds number $Re = Q\rho/(\mu b)$) (4). Practically, more than 85% of the surface is exposed to a homogenous wall shear stress for b/h > 20.

Equation [1] assumes steady flow, but is also used to estimate the average and maximum wall shear stress in dynamic flow regimes. Flow frequencies employed in stimulation of cells generally remain below 10 Hz (5-7), but physiological fluid flow might involve much higher frequencies. For example, small strains (< 10 με) in bone show strain information extending to 40 Hz (8). Theoretical extrapolation predicts that strain induced flow in bone elicits shear stresses up to 3 Pa for 100-200 με at 20-30 Hz (9). Blood flow also involves dynamic regimes with non-negligible higher harmonics: the spectral content of flow in the abdominal aorta of dogs, for example, shows frequencies reaching 80 Hz (10). High frequency modes have been shown to be stimulative to cells despite their small amplitudes; thus, fluid flow studies should be extended also to this range. It is questionable, though, if [1] is valid also for *dynamic* flows in PPFCs. Indeed, a dichotomy in oscillating flow regimes is reported for parallel-plate systems, characterized by the Womersley number W_o (= $\sqrt{(\omega/\nu)}\, L_c$, where $\omega = 2\pi f$, f = flow frequency, ν = kinematic viscosity, L_c = characteristic length; (11, 12)); this explicitly points at a limitation for the use of PPFCs under high frequency regimes.

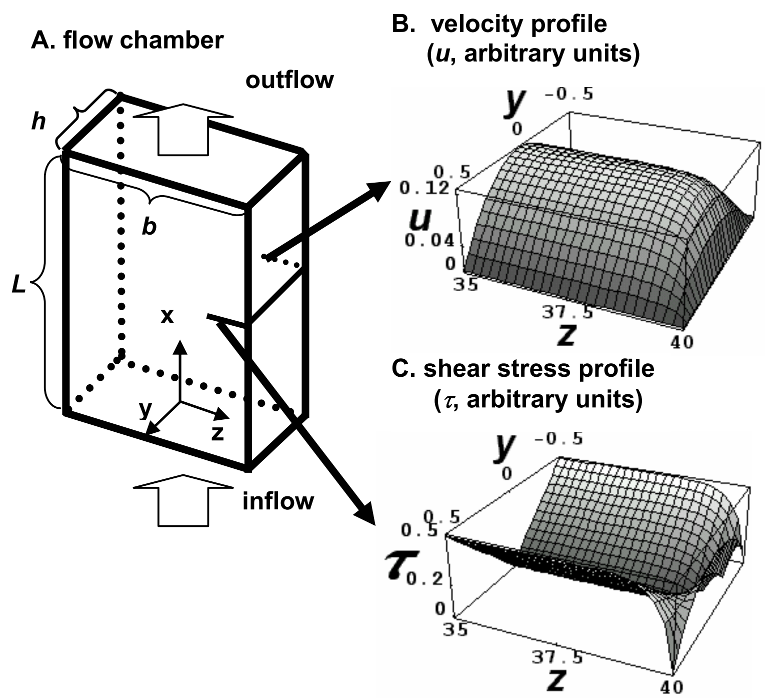

Figure 1. The flow chamber and its velocity and shear stress profile in arbitrary units. A. Diagram of a parallel-plate flow chamber of width *b,* height *h*, and length *L*, in its orientation in the *x-y-z* axes. The fluid is forced through the chamber by a steady pressure gradient along the *x-axis*. (b) and (c) show the calculated velocity profile *u* and the shear stress profile *τ*, respectively, for an aspect ratio b/h = 80. The arrows indicate that the profiles were taken very near the right edge of the flow chamber. The shear stress has its maximum value at the plate surfaces and vanishes at the chamber corners. Parabolic velocity profile and homogenous wall shear stress are characteristic for steady flow between parallel plates.

The aim of this paper is to characterize PPFCs for high frequency flow regimes, and to determine how eventual limitations can be reduced. We derived a relationship between the wall shear stress and flow, as well as between flow and pressure gradient under oscillating regimes, generalized to include higher harmonics.

MATHEMATICAL MODEL

Dynamic flow

The mathematical model assumes a laminar flow of a Newtonian fluid under isothermal conditions and imposes a no-slip boundary condition. The pressure gradient over the PPFC has a steady component γ and an oscillating component γ_o of frequency *f*. The Navier-Stokes equation is then:

$$\rho \frac{\partial u}{\partial t} - \mu \frac{\partial^2 u}{\partial y^2} = \gamma + \gamma_o \sin(\omega t) \qquad [2]$$

where velocity field *u* is a function of *y* and time variable *t.* The principle of superposition implies a generalization to dynamic flow regimes with higher harmonics. The solution of the velocity field has the form (Appendix [A.1-4]; (13)):

$$u(y,t) = C_1(y) + C_2(y)Cos(\omega t) + C_3(y)\sin(\omega t) \qquad [3]$$

In order to formulate the relations between the wall shear stress, the flow, and the pressure gradient, we introduce two dimensionless scaling factors: shear factor *T* and flow factor *K*, respectively.

**Shear factor *T(h/λ*

The oscillating wall shear stress component is related to flow amplitude q_o, chamber width b, height h, and viscous penetration depth λ_v ($=\sqrt{(2\nu/\omega)}$; ν = ratio of fluid viscosity to fluid mass density; $\omega = 2\pi f$) as:

$$\tau_{wo}(t) = q_o \frac{\mu}{bh^2}\left(\frac{h/\lambda_v}{cc_+(h/\lambda_v)}\right)\left(\sqrt{\frac{\sin^2(h/\lambda_v)+\sinh^2(h/\lambda_v)}{1-2(\lambda_v/h)\dfrac{ss_+(h/\lambda_v)}{cc_+(h/\lambda_v)}-2(\lambda_v/h)^2\dfrac{cc_-(h/\lambda_v)}{cc_+(h/\lambda_v)}}}\right)\sin(\omega t+\psi) \qquad [4]$$

We simplify [4] by introducing shear factor T(h/λ_v) including all functions with the argument h/λ_v, to scale the oscillating wall shear stress amplitude. The total wall shear stress τ_{wt} solution of [2] is then:

$$\tau_{wt}(t) = \frac{6\mu}{bh^2}Q_o\left(1 \pm \frac{q_o}{Q_o}T(h/\lambda_v)\sin(\omega t+\psi)\right) \qquad [5]$$

where Q_o is the steady flow component and ψ is the phase difference between wall shear stress and flow. Figure 2 shows the velocity profile variations for various frequencies.

$T(h/\lambda_v)$ (Appendix [A.11]) is close to unity when the wall shear stress is proportional to flow, *i.e.*, when $h/\lambda_v < 2$ (Figure 3a). From [5] and [1], the oscillating wall shear stress amplitude becomes $6\mu QT/(bh^2)$. The critical frequency 11.2 Hz is calculated at $h/2 = \lambda_v$, using the fluid physical properties of the culture medium and h = 0.3 mm (Figure 2). Decreasing h increases the critical frequency (Figures 3b,c), increasing h demands increasing the fluid viscosity μ (Figure 3d). The physical properties of the fluid (μ, ρ), and the distance between the plates (h) determine the critical frequency f_c:

$$\left(\sqrt{\left(\frac{\rho\pi f_c}{\mu}\right)}\right)h = 2 \Rightarrow f_c = \frac{4\mu}{\rho\pi h^2} \qquad [6]$$

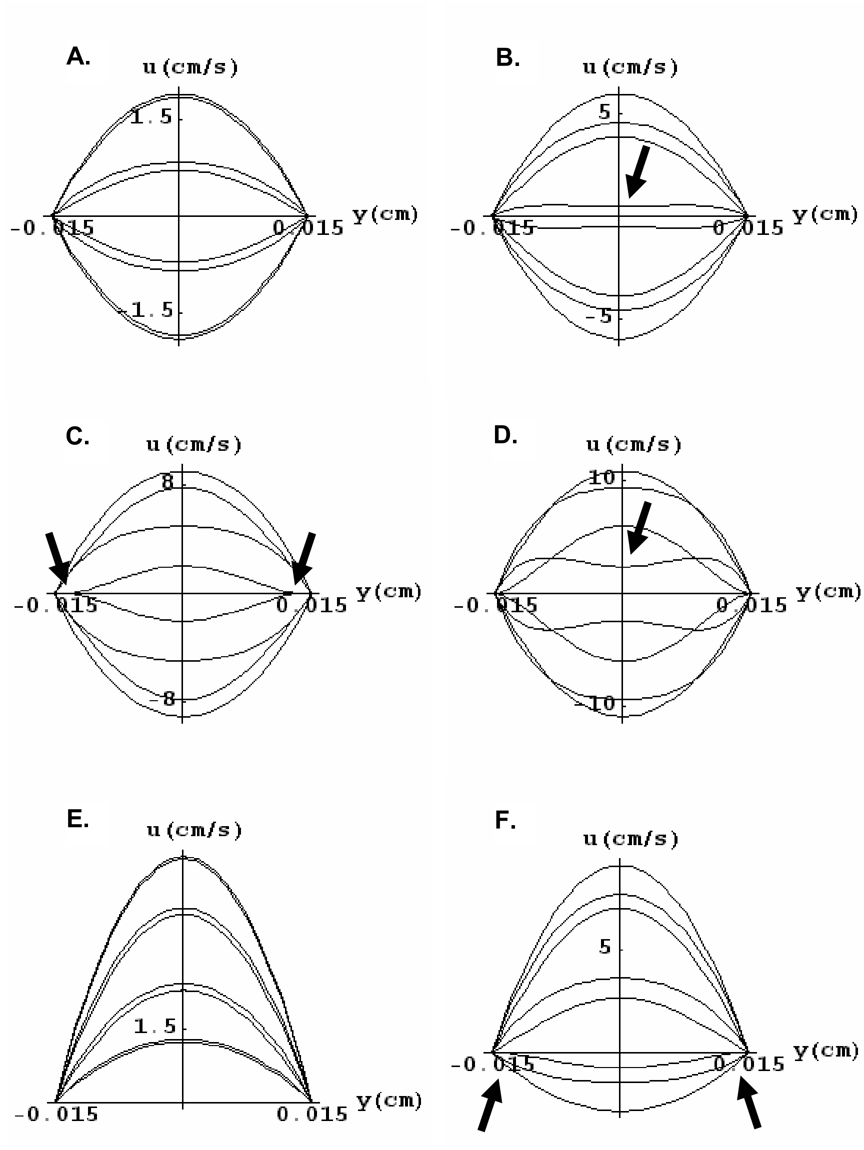

Figure 2. The velocity profiles in one cycle of oscillation. The graphs show the velocity profiles at time intervals an 8th part of the corresponding period. We simulated a typical cell culture medium (Dulbeccos' Modified Eagle Medium (DMEM) with supplements, viscosity = 0.0078 poise, density = 0.99 g/cm^3, at 37^{o}C), subjected to a flow amplitude of 0.15 ml/s between plates separated by 0.03 cm. A. The velocity profiles at 5 Hz, exhibit *quasi-parabolic form* throughout one flow cycle. B. At a frequency of 11.2 Hz, the quasi-parabolic velocity profile breaks down by an *arching* between the plates (arrow). At higher frequencies, *arching*, occurs near the plates (20 Hz, C), or between the plates (44.8 Hz, D). E and F show the velocity profiles at 5 Hz and 11.2 Hz respectively, imposed upon a steady flow component. Note that the symmetry about the y-axis is lost due to the steady flow component. However, the *quasi-parabolic form* of the velocity profile still breaks down at 11.2 Hz as indicated by the arrows in F. Quasi-parabolic velocity profile, indicative of quasi-steady flow breaks down when the flow frequency is above 11.2 Hz for the given fluid properties and chamber dimensions.

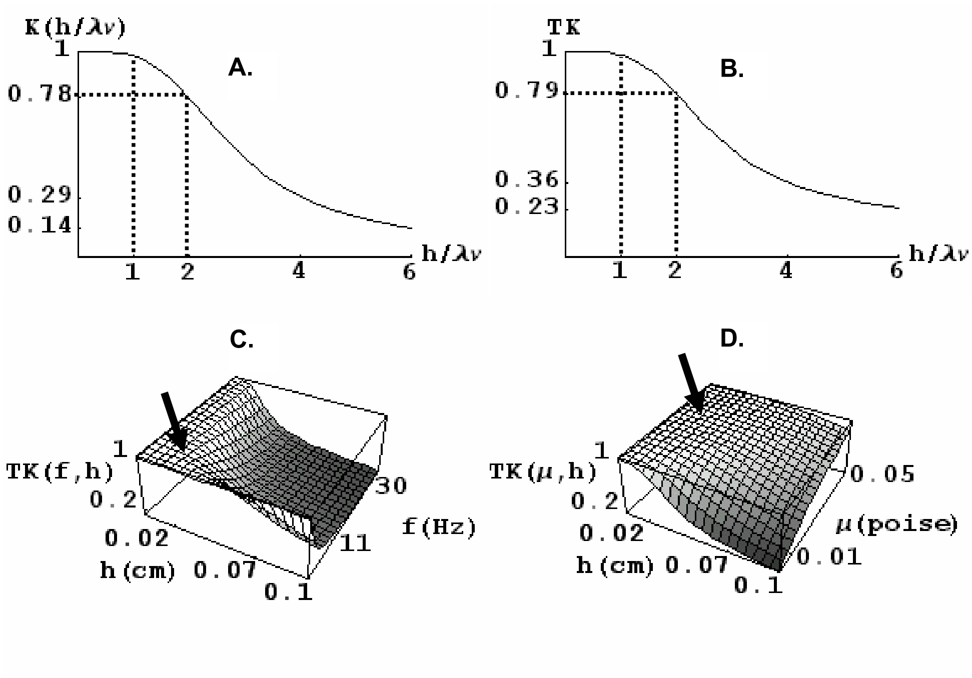

Figure 3. The shear factor. A. The shape of the shear factor (Appendix (A.11)) distinguishes a dichotomy in flow regimes separated by $h/\lambda_v = 2.0$. B. For a typical cell culture medium (DMEM, with supplements) the $T(h/\lambda_v)$ curve digresses from unity depending on the value of h. C. shows that the critical frequency can be raised by minimizing h while keeping $T(h/\lambda_v)$ close to unity for DMEM. D. Shows that the fluid viscosity μ can be increased (from 0.005 poise, assuming that ρ is not significantly changed) while keeping $T \sim 1.0$, even at higher h values up to about 1 mm. In both C and D, the arrow indicates the region where $T \sim 1.0$ i.e., where $h/\lambda_v < 2$ validating the adaptation of equation (1) for dynamic flow.

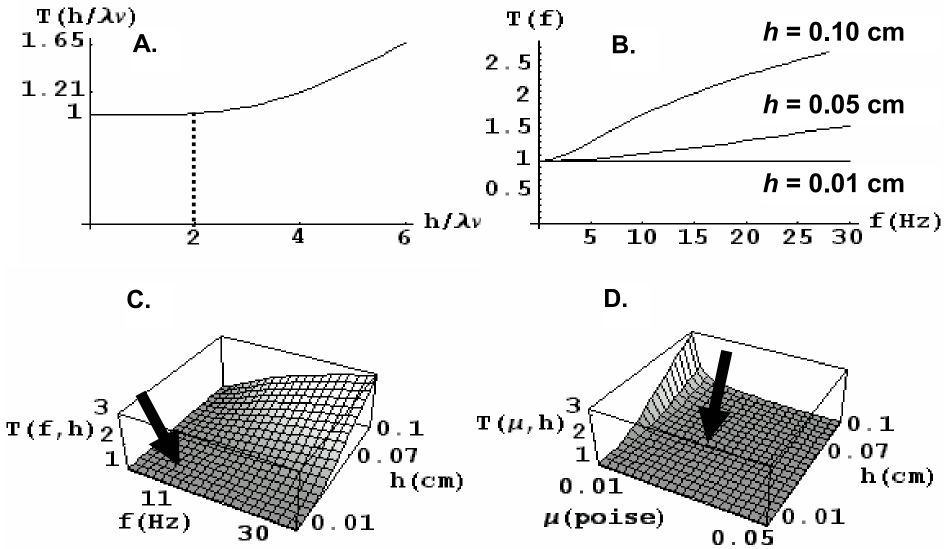

Figure 4. The flow factor. A. The flow factor $K(h/\lambda_v)$ (Appendix (A.12)) varies from unity by 2% at h/λ_v = 1.0 and drops to 0.78 at h/λ_v = 2.0. B. The product between the flow and shear factor is asymptotic to the horizontal axis. $T(h/\lambda_v)K(h/\lambda_v)$ scales the wall shear stress when the oscillating pressure gradient amplitude is kept constant as h/λ_v is varied ($TK = 0.79$ when $\alpha h = 2$). A and B illustrate that varying h/λ_v while keeping the pressure gradient amplitude constant leads to a lowering of the initial wall shear stress compared to its value if the flow were steady. C. *TK* drops faster at higher values of *h* and *f*. D. shows that *TK* drops faster for lower values of μ and higher *h*. In both C and D*,* the arrow indicates the region where *TK* ~1.0, *i.e.,* $h/\lambda_v < 1$. Equation (1) is valid for $h/\lambda_v < 2$ provided that the flow measurement is simultaneous to the change in h/λ_v parameters.

Flow factor $K(h/\lambda_v)$

The oscillating flow amplitude q_o can be scaled by a flow factor $K(h/\lambda_v)$ in relation with the oscillating pressure gradient amplitude γ_o:

$$q_o = \frac{bh^3\gamma_o}{12\mu}K(h/\lambda_v) \qquad [7]$$

K (Appendix [A.12]) is a decreasing function of h/λ_v (Figure 4). This shows that pressure gradient drops for $h/\lambda_v > 1$, which means that the wall shear stress is underestimated for $h/\lambda_v > 1$. For example, there is an overestimation of the magnitude of the wall shear stress by 21% at the critical frequency ($h/\lambda_v = 2$). In order to correct for that, the oscillating wall shear stress amplitude has to be scaled by the product TK when the oscillating pressure gradient amplitude is kept constant:

$$\frac{6\mu q_o}{bh^2}K(h/\lambda_v)T(h/\lambda_v) \qquad [8]$$

So, [8] should be used in experimental set-ups in which the pressure gradient is controlled, because the resulting shear stress is underestimated. The wall shear stress is linear to flow when $h/\lambda_v < 2$ but the flow is linear with the pressure gradient when $h/\lambda_v < 1$.

Higher harmonic modes

The flow profile may show a more arbitrary shape depending on the type of pump mechanism used. When the flow is periodic, it can be expanded into a Fourier series (see [A.10]), and from [5] follows:

$$\tau(t) = \frac{6\mu}{bh^2}\left\{Q_o + \sum_{n=1}^{m} T_n\left[q_n^c\cos((2\pi f_o n)t + \psi_n^c) + q_n^s\sin((2\pi f_o n)t + \psi_n^s)\right]\right\} \qquad [9]$$

where ψ is the phase difference between the wall shear stress and the corresponding flow component at the given indices. Shear factor T is discretized due to the form of the angular frequency ($\omega_n = 2\pi f_o n$, *for* n = 1,2,3...). The summation limit m imposes that for $n > m$, flow coefficients q_n^c or q_n^s become negligible compared to the average flow. To apply a flow regime such that $h/\lambda_v < 2$ for all harmonics, the highest harmonic mode ($f_o m$) must be less than the critical frequency f_c.

DISCUSSION

For dynamic regimes in a PPFC, the relations between wall shear stress, flow, and pressure gradient, were derived using dimensionless scaling factors $T(h/\lambda_v)$ and $K(h/\lambda_v)$. The dimensionless parameter h/λ_v was the key for establishing quasi-steady flow in laminar regimes. The analysis was expanded to apply for arbitrary dynamic laminar flows, identifying the limits for the highest harmonic mode of the flow.

To establish laminar quasi-steady flow under dynamic regimes in PPFCs, the following conditions apply: 1) $h/\lambda_v < 2$ based on the consequent *quasi-parabolic* form of the velocity profile, and 2) $f_o < f_c / m$, where the *criticial frequency* f_c is the upper threshold for this flow regime and m is the highest harmonic of flow. Quasi-steady flow means that the dynamic wall shear stress follows the changing flow linearly. When the flow is beyond the quasi-steady regime, there will be less oscillation due to backflow (figure 2 b-d), but shearing might increase at the plate walls since the shear factor $T(h/\lambda_v) > 1$ (Figure 3, [5]).

Attached cells occupy < 4.1% of the chamber height, based on unsheared endothelial monolayers (3.4±0.7 μm, see (14); for h = 100-300 μm). Since the wall shear stress is estimated by average parameters (flow or pressure gradient), assumption of smooth rigid walls is reasonable. The Reynolds and the Womersley numbers empirically predict the transition from laminar to turbulent oscillating flow. Measurement on a dog's blood vessel relates the maximum Re to 150-250 times W_o (11). The transition to turbulent flow is reached at $Re < 2640$ (15), however, values as low as $Re \sim 1000$ have been found experimentally. Assuming that the transition to turbulent flow for flow between parallel-plates is $Re = 2000$, this transition occurs at a supplementary condition: $h/\lambda_v = 8/\sqrt{2} \approx 5.7$. The flow regime where $h/\lambda_v < 2$, is far from turbulence provided the fluid properties remain stable.

Our findings provide guidelines in adapting the PPFC in terms of parameters in h/λ_v for investigating cell mechanosensitivity *in vitro*. Using the PPFC, the effect of physiological flow regimes on cells can be studied involving a wide range of frequencies, types of viscous fluids, and values for h that approximate actual shearing flow in various anatomical sites, such as blood vessels or the lacuno-canalicular network in bone.

ACKNOWLEDGEMENTS

This work was supported by funds from the Space Research Organization of The Netherlands (SRON), project number: MG-055. We thank Dr. Mathieu Pourquie (Delft University of Technology, Delft, The Netherlands) for his contribution in numerically testing some of our analytical results.

REFERENCES

1. Brown TD 2000 Techniques for mechanical stimulation of cells in vitro: a review. J Biomech 33(1):3-14.

2. Belansky R, Wanser K 1993 Laser Doppler velocimetry using a bulk optic Michelson interferometer: A student laboratory experiment. Am J Phys 61(11):1014-1019.

3. Booij W, de Jongh A, de Mul F 1995 Flow profile study using miniature laser-doppler velocimetry. Am J Phys 63(11):1028-1033.

4. Schlichting H 1968 Boundary layer theory, McGraw-Hill, New York.

5. Frangos JA, Eskin SG, McIntire LV, Ives CL 1985 Flow effects on prostacyclin production by cultured human endothelial cells. Science 227(4693):1477-1479.

6. Jacobs CR, Yellowley CE, Davis BR, Zhou Z, Cimbala JM, Donahue HJ 1998 Differential effect of steady versus oscillating flow on bone cells. J Biomech 31(11):969-976.

7. Klein-Nulend J, Semeins CM, Ajubi NE, Nijweide PJ, Burger EH 1995 Pulsating fluid flow increases nitric oxide (NO) synthesis by osteocytes but not periosteal fibroblasts--correlation with prostaglandin upregulation. Biochem Biophys Res Commun 217(2):640-648.

8. Fritton SP, McLeod J, Rubin CT 2000 Quantifying the strain history of bone: spatial uniformity and self-similarity of low-magnitude strains. J Biomech 33(3):317-325.

9. Weinbaum S, Cowin SC, Zeng Y 1994 A model for the excitation of osteocytes by mechanical loading-induced bone fluid shear stresses. J Biomech 27(3):339-360.

10. Newman DL, Sipkema P, Greenwald SE, Westerhof N 1986 High frequency characteristics of the arterial system. J Biomech 19(10):817-824.

11. Loudon C, Tordesillas A 1998 The use of the dimensionless Womersley number to characterize the unsteady nature of internal flow. J Theoret Biol 191(1):63-78.

12. Yakhot A, Arad M, Ben Dor G 1999 Numerical investigation of a laminar pulsating flow in a rectangular duct. Internat J Numer Meth Fluids 29(8):935-950.

13. Landau LD, Lifshitz EM 1959 Fluid Mechanics, Permagon Press, Reading, MA.

14. Barbee KA, Davies PF, Lal R 1994 Shear stress-induced reorganization of the surface topography of living endothelial cells imaged by atomic force microscopy. Circ Res 74(1):163-171.

15. Orszag SA, Patera AT 1983 Secondary Instability of Wall-bounded Shear Flows. J Fluid Mech 128:347-385.

APPENDIX

The velocity profile for dynamic flow between parallel plates takes the form of equation [3] with:

$$C_1(y) = -\frac{\gamma}{2\mu}(y^2 - \frac{h^2}{4}) \quad \text{[A.1]}$$

$$C_2(y) = \frac{\gamma_o}{\rho\omega}\left[\frac{CC[\frac{1}{\lambda_v}(-y+h/2), \frac{1}{\lambda_v}(y+h/2)] + CC[\frac{1}{\lambda_v}(y+h/2), \frac{1}{\lambda_v}(-y+h/2)]}{cc_+(\frac{h}{\lambda_v})} - 1\right] \quad \text{[A.2]}$$

$$C_3(y) = \frac{\gamma_o}{\rho\omega}\left[\frac{SS[\frac{1}{\lambda_v}(-y+h/2), \frac{1}{\lambda_v}(y+h/2)] + SS[\frac{1}{\lambda_v}(-y+h/2), \frac{1}{\lambda_v}(y+h/2)]}{cc_+(\frac{h}{\lambda_v})}\right] \quad \text{[A.3]}$$

where the following functions were defined:

$$\begin{aligned} SS(x_1, x_2) &= \sin(x_1)\sinh(x_2) \\ CC(x_1, x_2) &= \cos(x_1)\cosh(x_2) \\ ss_\pm(x) &= \sin(x) \pm \sinh(x) \\ cc_\pm(x) &= \cos(x) \pm \cosh(x) \end{aligned} \quad \text{[A.4]}$$

The phase difference between the velocity of a fluid layer and the pressure gradient is:

$$\sigma = \tan^{-1}(\frac{C_2(y)}{C_3(y)}) \quad \text{[A.5]}$$

when the velocity profile takes the form:

$$u(y,t) = C_1(y) + \sqrt{C_2(y)^2 + C_3(y)^2}\sin(\omega t + \sigma) \quad \text{[A.6]}$$

The oscillating wall shear stress calculated from the gradient of the velocity is then:

$$\tau_{wo} = \gamma_o \frac{\mu\alpha}{\rho\omega}\frac{\sqrt{ss_-^2(h/\lambda_v) + ss_+^2(h/\lambda_v)}}{cc_+(h/\lambda_v)}\sin(\omega t + \vartheta) \quad \text{[A.7]}$$

where the phase difference is:

$$\vartheta = \tan^{-1}\left(\frac{\frac{d}{dy}C_2(y)}{\frac{d}{dy}C_3(y)}\right)_{y=\pm\frac{h}{2}} = \tan^{-1}\left(\frac{ss_-(h/\lambda_v)}{ss_+(h/\lambda_v)}\right) \quad \text{[A.8]}$$

For an expression when the oscillating wall shear stress is related with the flow (see equation (4)), the phase difference is:

$$\psi = \tan^{-1}\left(\frac{\int_{-h/2}^{h/2} C_2(y)dy}{\int_{-h/2}^{h/2} C_3(y)dy}\right) = \tan^{-1}\left(\frac{\alpha h\left(cc_+(h/\lambda_v)\right) - ss_+(h/\lambda_v)}{ss_-(h/\lambda_v)}\right) \qquad [A.9]$$

A smooth periodic continuous flow can be expanded into its Fourier series with an upper index indicating a “hard” limit giving a series termination at *m*, or a “soft” limit giving negligible terms after *m*:

$$Q(t) = Q_o + \sum_{n=1}^{m}\left[q_n^c \cos(2\pi f_o nt) + q_n^s \sin(2\pi f_o nt)\right] \qquad [A.10]$$

The shear factor $T(h/\lambda_v)$ and the flow factor $K(h/\lambda_v)$, are derived from (A.7):

$$T(h/\lambda_v) = \frac{1}{6}\left(\frac{h/\lambda_v}{cc_+(h/\lambda_v)}\right)\left(\sqrt{\frac{\sin^2(h/\lambda_v) + \sinh^2(h/\lambda_v)}{1 - 2(\lambda_v/h)\dfrac{ss_+(h/\lambda_v)}{cc_+(h/\lambda_v)} - 2(\lambda_v/h)^2\dfrac{cc_-(h/\lambda_v)}{cc_+(h/\lambda_v)}}}\right) \qquad [A.11]$$

$$K(h/\lambda_v) = \frac{6}{(h/\lambda_v)^2}\left(1 - \frac{2}{(h/\lambda_v)}\right)\left(\frac{ss_+(h/\lambda_v)}{cc_+(h/\lambda_v)}\right) \qquad [A.12]$$

LIST OF SYMBOLS

γ = constant pressure gradient component for dynamic fluid flow

γ_o = amplitude of the oscillating pressure gradient component for dynamic flow

ϑ = phase difference between the oscillating wall shear stress and the oscillating pressure gradient

h/λ_v = viscous penetration depth

μ = fluid viscosity

$\mu\in$ = microstrain

ν = kinematic viscosity

ρ = fluid density

σ = phase difference between the velocity and the oscillating pressure gradient

τ_w = wall shear stress for steady flow

τ_{wo} = oscillating wall shear stress

τ_{wt} = total wall shear stress for dynamic flow

τ = fluid shear stress

ψ = phase difference between the wall shear stress and the oscillating flow

$\omega = 2\pi f$ = angular frequency

∇ = del operator

∇^2 = Laplacian operator

A_n = velocity field amplitudes in the summation term of the steady flow solution

b = PPFC width

c_n = velocity field function arguments in the summation term of the steady flow solution

f = flow frequency

f_c = critical frequency

F = external force density term

h = distance between the plates

K = flow factor

L = wetted length of the flow chamber

m = highest frequency mode

Pa = Pascal

p = pressure

q_o = amplitude of the oscillating flow component

Q *or* Q_o = flow

Re = Reynolds number

T = shear factor

u = velocity field

W_o = Wormesley number

x = length axis

y = height axis

z = width axis